Single-Channel Kinetic Analysis of Chimeric $\alpha7$–5HT$_{3A}$ Receptors

Diego Rayes, Guillermo Spitzmaul, Steven M. Sine, and Cecilia Bouzat

Instituto de Investigaciones Bioquimicas, Universidad Nacional del Sur–Consejo Nacional de Investigaciones Científicas y Técnicas, Bahia Blanca, Argentina (D.R., G.S., C.B.); and Receptor Biology Laboratory, Department of Physiology and Biomedical Engineering, Mayo Clinic College of Medicine, Rochester, Minnesota (S.M.S.)

ABSTRACT

The receptor chimera $\alpha7$–5HT$_{3A}$ has served as a prototype for understanding the pharmacology of $\alpha7$ neuronal nicotinic receptors, yet its low single channel conductance has prevented studies of the activation kinetics of single receptor channels. In this study, we show that introducing mutations in the M3–M4 cytoplasmic linker of the chimera alters neither the apparent affinity for the agonist nor the EC$_{50}$ but increases the amplitude of agonist-evoked single channel currents to enable kinetic analysis. Channel events appear as single brief openings flanked by long closings or as bursts of several openings in quick succession. Both the open and closed time distributions are described as the sum of multiple exponential components, but these do not change over a wide range of acetylcholine (ACh), nicotine, or choline concentrations. Bursts elicited by a saturating concentration of ACh contain brief and long openings and closings, and a cyclic scheme containing two open and two closed states is found to adequately describe the data. The analysis indicates that once fully occupied, the receptor opens rapidly and efficiently, and closes and reopens several times before it desensitizes. Channel closing and desensitization occur at similar rates and account for the invariant open and closed time distributions.

The Cys-loop superfamily of neurotransmitter receptors includes receptors activated by acetylcholine (ACh), GABA, glycine, and 5-HT. Each of these neurotransmitters activates a corresponding pentameric receptor composed of identical subunits (i.e., a homopentamer). Because homopentameric receptors diverged least from the common ancestral receptor, they are expected to share fundamental mechanisms common to all members of the receptor superfamily and thus serve as prototypes. The homomeric $\alpha7$ ACh receptor contributes to a wide range of neurophysiological processes, has been implicated in neurological diseases, and is a target for pharmacological agents (Gotti and Clementi, 2004). Nevertheless, little is known about the mechanism by which ACh activates $\alpha7$ receptors, mainly because they are difficult to express in mammalian cells. The limited cell surface expression was traced to decreased palmitoylation of $\alpha7$ (Drisdel et al., 2004); more recently, however, the chaperone protein ric-3 was found to promote cell-surface expression. As a result, ACh-evoked whole cell currents have been recorded from human embryonic kidney cells coexpressing $\alpha7$ and ric-3 (Williams et al., 2005), but single channel currents have not been reported. Furthermore, although $\alpha7$ receptors express in oocytes, few studies have reported single-channel currents, and analysis of single channel current kinetics has not been reported. In addition, several conductance states of channels were observed in both wild-type and mutant $\alpha7$ AChRs expressed in oocytes (Palma et al., 1999; Fucile et al., 2000), complicating kinetic analysis.

Chimeric receptors, composed of $\alpha7$ sequence from the N terminus to the start of M1 followed by 5HT$_{3A}$ receptor sequence, form functional homopentameric receptors when expressed in mammalian cells (Eisele et al., 1993). For nearly a decade, the $\alpha7$–5HT$_3$ chimera has served as a prototype for investigating the pharmacology of homomeric α_7 receptors, but its unitary conductance is too low to allow direct detection of single channel currents. However, by substituting neutral or negatively charged residues for three arginines in the cytoplasmic linker spanning the M3 and M4 domains (Kelley et al., 2003), we were able to resolve ACh-evoked single channel currents (Bouzat et al., 2004). We report here the kinetic analysis of currents through $\alpha7$–5HT$_3$ receptors and suggest that the $\alpha7$–5HT$_3$ chimera with increased conductance is a good model for studying the molecular pharmacology of homomeric Cys-loop receptors.

ABBREVIATIONS: ACh, acetylcholine; 5-HT$_{3A}$, serotonin type 3A; BTX, α-bungarotoxin; LC, low conductance; HC, high conductance.

Materials and Methods

Site-Directed Mutagenesis and Expression of α7–5HT₃ Receptors. Mutant subunits were constructed using the QuikChange site-directed mutagenesis kit (Stratagene, Inc., La Jolla, CA). To increase unitary conductance for single-channel recordings, we mutated three arginine residues responsible for the low conductance of the serotonin type 3A receptor (5-HT$_{3A}$) as follows: R432Q, R436D, and R440A (Kelley et al., 2003). Mutant subunits were confirmed by restriction enzyme analysis and sequencing. BOSC cells were transfected with α7–5HT₃ subunit cDNAs using calcium phosphate precipitation, as described previously (Bouzat et al., 1994, 2000). A plasmid encoding green fluorescent protein (pGreen lantern) was also included to allow identification of transfected cells under fluorescence optics. Cells were used for single-channel measurements 1 or 2 days after transfection.

Steady-State ACh Binding. Transfected cells were harvested by gentle agitation in phosphate-buffered saline, centrifuged at 1000g for 1 min, and re-suspended in potassium Ringer's solution (140 mM KCl, 5.4 mM NaCl, 1.8 mM CaCl$_2$, 1.7 mM MgCl$_2$, 25 mM HEPES, 30 mg/liter bovine serum albumin, adjusted to pH 7.4 with 10 to 11 mM NaOH). Agonist binding was determined by competition of specified concentrations of ACh against the initial rate of ^{125}I-α-bungarotoxin (BTX) binding as described previously (Sine et al., 1995). The total number of binding sites was determined by incubating cells with 25 nM ^{125}I-α-BTX for 1 h and subtracting a blank determined in the presence of 10 μM α-BTX (Quiram and Sine, 1998). After computing fractional occupancy from the initial rates of toxin binding (Sine and Taylor, 1979), the following equation was fitted to the data: 1-fractional occupancy = $1 - [L]^{n_H}/([L]^{n_H} + K^{n_H})$, where [L] is agonist concentration, K is the apparent dissociation constant, and n_H is the Hill coefficient.

Single-Channel and Macroscopic Patch-Clamp Recordings. Single-channel recordings were obtained in the cell-attached configuration (Hamill et al., 1981) at a membrane potential of -70 mV and at 20°C. The bath and pipette solutions contained 142 mM KCl, 5.4 mM NaCl, 0.2 mM CaCl$_2$, and 10 mM HEPES, pH 7.4. Solutions free of magnesium and with low-calcium were used to minimize channel block by divalent cations. Patch pipettes were pulled from 7052 capillary tubes (Garner Glass, Claremont, CA) and coated with Sylgard (Dow Corning, Midland, MI). Pipette resistances ranged from 5 to 7 MΩ. Agonists [ACh, (±)-nicotine, and choline (Sigma, St. Louis, MO)] were added to the pipette solution.

Single-channel currents were recorded using an Axopatch 200 B patch-clamp amplifier (Molecular Devices, Sunnyvale, CA), digitized at 5-μs intervals with the PCI-6111E interface (National Instruments, Austin, TX), recorded to the computer hard disk using the program Acquire (Bruxton Corporation, Seattle, WA), and detected by the half-amplitude threshold criterion using the program TAC 4.0.10 (Bruxton Corporation) at a final bandwidth of 10 kHz (Gaussian digital filter). Open- and closed-time histograms were plotted using a logarithmic abscissa and a square root ordinate (Sigworth and Sine, 1987) and fitted to the sum of exponential functions by maximum likelihood using the program TACFit (Bruxton Corporation, Seattle, WA). The K_d for fast blockade by the agonist was calculated according to the equation: $I_o/I_b = 1 + [B]/K_d$, where I_o is the current in the absence of blockade, I_b is the current at different concentrations of blocker (agonist), [B] is the blocker concentration, and K_d is the dissociation equilibrium constant for binding to the blocking site (Sine and Steinbach, 1984; Grosman and Auerbach, 2000).

For outside-out patch or whole-cell recordings, the pipette solution contained 140 mM KCl, 5 mM EGTA, 5 mM MgCl$_2$, and 10 mM HEPES, pH 7.3. Extracellular solution contained 150 mM NaCl, 5.6 mM KCl, 0.2 mM CaCl$_2$, and 10 mM HEPES, pH 7.3. Outside-out patches were moved into position at the outflow of a perfusion system as described before (Liu and Dilger, 1991; Spitzmaul et al., 2001). A series of applications of extracellular solution-containing agonists was applied to the patch. The time of application was 1 and 0.5 s for outside-out and whole-cell recordings, respectively. The time of acquisition was 2 s. Macroscopic currents were filtered at 5 kHz, digitized at 20 kHz, and stored on hard disk. Data analysis was performed using the IgorPro software (WaveMetrics Inc., Lake Oswego, Oregon). The ensemble mean current was calculated for five to ten individual current traces.

For calculation of the EC$_{50}$, macroscopic responses were recorded at different agonist concentrations and at the end of the experiment loss of channel activity was assessed to discard results from patches with excessive rundown. If the maximum peak current decreased by more than 85%, the whole experiment was discarded.

Mean currents were usually fitted by a single exponential function: $I_{(t)} = I_0 \exp(-t/\tau_d) + I_\infty$, where I_0 and I_∞ are the peak and the steady-state current values, respectively, and τ_d is the decay time constant. Current records were aligned with each other at the point of the rising phase where the current reached 50% of maximum. EC$_{50}$ and Hill coefficients were calculated by nonlinear regression analysis using the Hill equation: $I/I_{max} = 1/[1 + (EC_{50}/L)^{n_H}]$, where EC$_{50}$ is the agonist concentration that elicits the half-maximal response, n_H is the Hill coefficient, and L is the agonist concentration. Desensitization onset and recovery rates were calculated by the following relationships: 1) observed desensitization rate = onset + recovery and 2) extent of desensitization = onset/(onset + recovery).

Kinetic Analysis. Kinetic analysis was performed as described before (Bouzat et al., 2000, 2002). The analysis was restricted to bursts of channel openings, each reflecting the activity of a single channel. Bursts were identified as a series of closely spaced events preceded and followed by closed intervals longer than a critical duration (τ_{crit}). This duration was taken as the point of intersection of the second and third closed components in the closed-time histogram. In general, burst resolution was about 2 ms. Only bursts containing more than three openings were considered for further analysis. Bursts start and finish with an opening event.

For each recording, kinetic homogeneity was determined by selecting bursts on the basis of distributions of mean open duration, mean closed duration, and open probability (Bouzat et al., 2000, 2002). In general, the distributions contained an approximately Gaussian component. Bursts showing mean open channel durations, mean closed channel durations, and open probabilities within 2 S.D. of the mean of the major component were selected. In most cases, more than 90% of bursts were selected (Bouzat et al., 2000).

The resulting open and closed intervals from single patches were analyzed according to kinetic schemes using an interval-based maximum likelihood algorithm that corrects for missed events and computes error limits of the fitted rate constants (Qin et al., 1996) [QuB suite (http://www.qub.buffalo.edu); State University of New York, Buffalo, NY)]. A dead time of 30 μs was imposed in all recordings. Probability density functions of open and closed durations were calculated from the fitted rate constants and instrumentation dead time and superimposed on the experimental dwell time histogram as described by Qin et al. (1996).

Results

Apparent Affinity and Dose-Response Relationship for the HC Form of α7–5HT$_{3A}$. Although chimeric α7–5HT$_{3A}$ receptors express well in mammalian cells, ACh-evoked single-channel currents are too small to be detected using the patch clamp. To overcome this limitation, we mutated three positively charged residues in the M3-M4 cytoplasmic linker to neutral or acidic residues. The analogous mutations in homomeric 5HT$_{3A}$ receptors enabled detection of unitary currents (Kelley et al., 2003) and, in α7–5HT$_{3A}$ receptors, increased the unitary conductance from undetectable to approximately 90 pS (Bouzat et al., 2004). To determine whether the conductance-enhancing mutations affect

functional properties of $\alpha7$–5HT$_{3A}$ receptors, we measured steady-state binding and macroscopic currents as a function of ACh concentration.

cDNAs encoding the low conductance (LC) and high conductance (HC) forms of the $\alpha7$–5HT$_{3A}$ chimera were transiently transfected in 293 human embryonic kidney cells, and the expressed receptors studied 2 to 3 days later. Competition of ACh against ^{125}I-labeled α-bungarotoxin binding to intact cells revealed apparent dissociation constants of 183 $\pm$ 12 μM ($n = 3$) and 143 $\pm$ 10 μM ($n = 3$) for the LC and HC forms of $\alpha7$–5HT$_{3A}$, respectively.

To determine the dose-response relationship for activation of the HC form of $\alpha7$–5HT$_{3A}$ receptors, we measured macroscopic currents using the whole-cell patch-clamp configuration (Fig. 1). All experiments were carried out in a magnesium-free, low calcium solution (0.2 mM Ca^{2+}) at a holding potential of -50 mV. ACh elicits robust inward currents that show apparent saturation, and the rate of rise increases with increasing ACh concentration. The agonists ACh, nicotine, and choline activate the receptor with EC$_{50}$ values of 198 μM, 54 μM, and 1.7 mM, respectively. The calculated Hill coeffi-

cients were 2.0, 1.9, and 2.1 for ACh, nicotine, and choline, respectively. For the LC form of $\alpha7$–5HT$_{3A}$, the EC$_{50}$ for ACh determined under identical conditions was 180 μM, showing that the mutations do not affect the activation properties of the receptor. Both the EC$_{50}$ and n_H are subject to error because the rate of agonist application is slow relative to the rates of activation and desensitization, which underestimates the peak current and overestimates the relative steady-state current (Papke and Thinschmidt, 1988). This may account for the variability in the reported EC$_{50}$ and n_H values for $\alpha7$ and $\alpha7$–5HT$_3$ receptors (Corringer et al., 1998; Grutter et al., 2003). However, because the experiments with wild-type and triple mutant $\alpha7$–5HT$_3$ receptors were performed under the same conditions, we conclude that activation is not substantially affected by the triple mutation.

Desensitization of the HC Form of $\alpha7$–5HT$_{3A}$. We next measured the kinetics of activation and desensitization after rapid application of a saturating concentration of ACh (1 mM). To ensure rapid and uniform application, we formed outside-out patches and rapidly perfused them with ACh (Liu and Dilger, 1991; Spitzmaul et al., 2001). Figure 2 shows
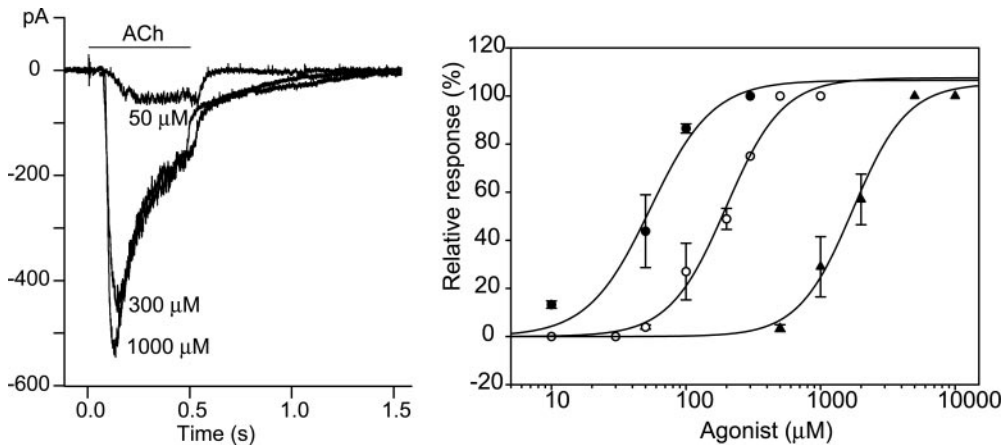
Fig. 1. Activation of $\alpha7$–5HT$_3$ (HC) receptors by agonists. Left, whole-cell currents evoked by application of the indicated concentrations of ACh. Bar shows time of ACh application. Right, dose-response relationship for activation by ACh ($\bigcirc$), nicotine ($\bullet$), and choline ($\blacktriangle$). The curves are fits to the Hill equation (see *Materials and Methods*).
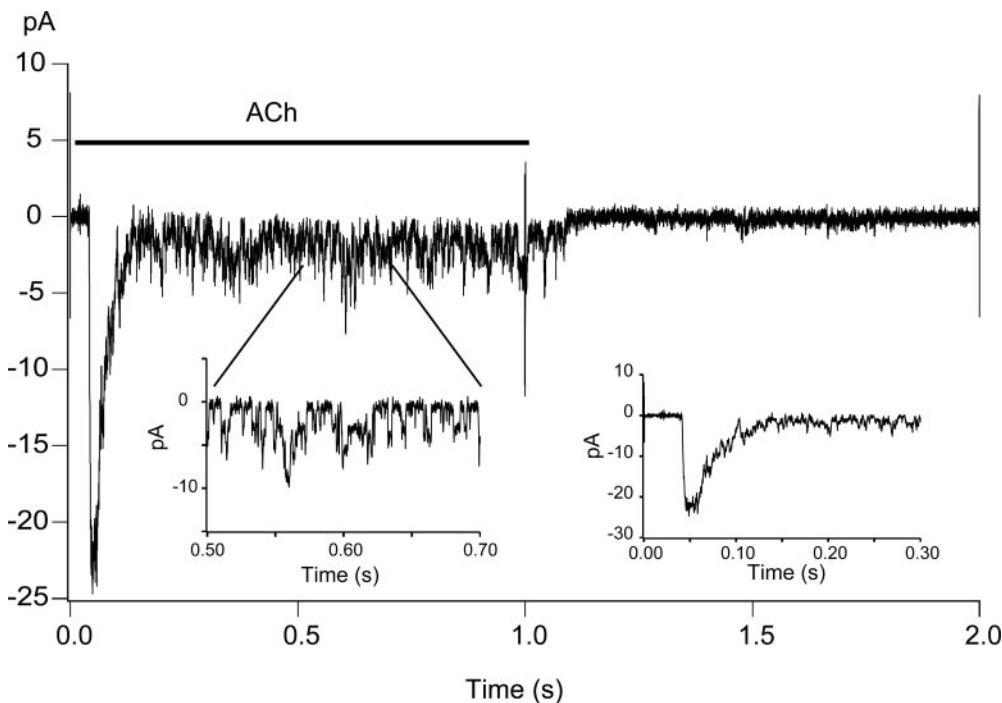
Fig. 2. Ensemble mean currents from $\alpha7$–5HT$_{3A}$ HC receptors obtained from an outside-out patch perfused with 1 mM ACh. Each trace represents the average response after five applications of agonist. The calculated decay time constant (τ_d) is 8 ms. The rise time in this patch is approximately 1 ms, similar to that measured with an open pipette perfused with saline. The steady-state current corresponds to 6.2% of that of the peak. Membrane potential, -50 mV. The bar indicates the application of ACh. The region between lines is expanded in the left inset to show unitary events corresponding to one of the five agonist applications. The inset in the right shows the rising phase of the current on an expanded time scale.

current recorded from a single outside-out patch to which ACh was rapidly applied. The current reaches a peak after approximately 0.5 to 1 ms and then decays as a result of desensitization. Fitting a single exponential function to the decay reveals a time constant τ_d of 8 ± 1.3 ms ($n = 3$). It is noteworthy that the current at steady state is not zero but fluctuates because of residual opening and closing of single receptor channels, amounting to 5 to 10% of the peak current. Rate constants for desensitization onset and recovery were determined by assuming a reversible two-state reaction between active and desensitized receptors during the course of current decay. The measured decay rate and fractional steady-state current yield a rate constant for onset of desensitization of approximately 110 s^{-1} and a rate constant for recovery from desensitization of approximately 10 s^{-1}.

The currents are seen to decay much more rapidly in outside-out patch recordings (Fig. 2) than in whole cell recordings (Fig. 1). This difference probably results from the faster and more uniform perfusion attainable for outside-out patches compared with entire cells (Niu et al., 1996; Sachs, 1999). Thus, our estimates of desensitization onset and recovery rates derive solely from outside-out patch experiments.

Agonist-Induced Channel Block of the HC Form of $\alpha7$–$5HT_{3A}$. Agonists themselves invariably block nicotinic receptor channels (Sine and Steinbach, 1984; Ogden and Colquhoun, 1985; Papke et al., 1988; Kem et al., 1997), and analysis of channel block is a prerequisite for analysis of single channel kinetics. We therefore examined single-channel currents activated by a range of high concentrations of

ACh, nicotine, and choline. All three agonists decrease the unitary current amplitude over a range of high concentrations. The ratio of current amplitude in the absence to that in the presence of block increases linearly for each agonist, yielding apparent dissociation constants for channel block of 40, 2.9, and 68 mM for ACh, nicotine and choline, respectively (Fig. 3). In addition to decreasing single-channel current amplitude, nicotine at concentrations greater than 300 μM, shows flickery block in which a fraction of the blocking events exceeds the instrument dead time, which shortens the mean open channel duration (see below). The shortening of open channel duration is accompanied by a systematic increase in the relative area of the briefest closed duration component, which increases from 0.29 ± 0.04 at 50 μM nicotine to 0.68 ± 0.05 at 3 mM.

Single Channel Kinetics of the HC Form of $\alpha7$–$5HT_{3A}$. When applied to cell-attached patches, a concentration of 30 μM ACh elicits infrequent single channel openings, but concentrations from 100 μM to 1 mM elicit robust channel activity (Fig. 4). For all concentrations of ACh, both the open and the closed time histograms are described by the sum of multiple exponential components. The open time constants are independent of ACh concentration and have the following average values: $\tau_1 = 130 \pm 17 \text{ }\mu$s, $\tau_2 = 1.1 \pm 0.3$ ms, and $\tau_3 = 6.9 \pm 1.9$ ms. The fractional areas of these components change between 30 and 100 μM ACh but show virtually no change between 100 μM and 1 mM (Fig. 4). At 30 μM ACh, the fractional area of the slowest open time component, τ_3 ($a_3 = 0.26 \pm$
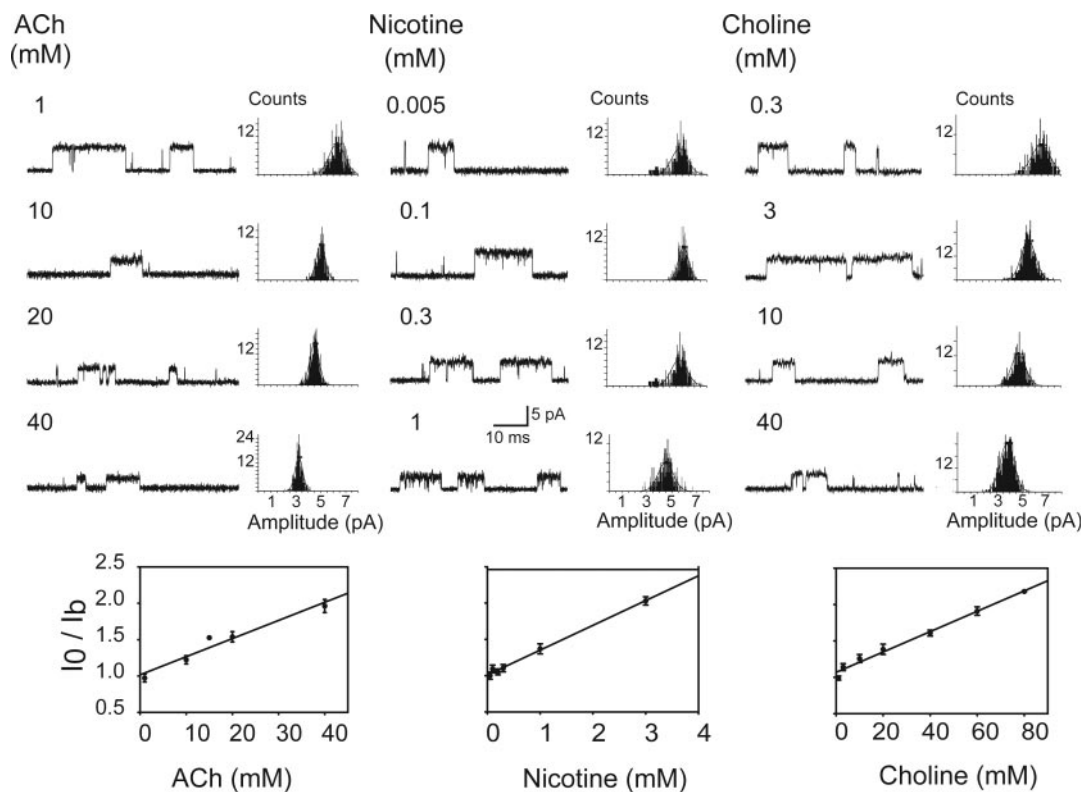
**Fig. 3.** Channel block by agonists. Top, $\alpha7$–$5HT_3$ channel traces at different agonist concentrations and the corresponding amplitude histograms are shown. Membrane potential, -70 mV. Bottom, relationship between the decrease in current and agonist concentration. I_o is the current at low agonist concentrations in the absence of channel block. I_b is the current at a given concentration of agonist.

0.08), is smaller than that obtained at concentrations between 50 μM and 3 mM ACh ($a_3 = 0.43 \pm 0.07$).

The temporal pattern of single channel currents for $\alpha7$–5HT$_{3A}$ HC receptors unexpectedly showed no clear dependence on the ACh concentration. This concentration independence is evident from inspection of single channel current traces, as well as from closed time histograms obtained across a range of ACh concentrations (Fig. 4). Two brief closed time components are systematically observed at all ACh concentrations, but their fractional areas (0.21 $\pm$ 0.05 and 0.15 $\pm$ 0.09) and mean durations (35 $\pm$ 10 μs and 550 $\pm$ 210 μs) are independent of ACh concentration. The succeeding closed time components also show no systematic dependence on ACh concentration. Thus, the temporal pattern of

single-channel currents through $\alpha7$–5HT$_{3A}$ HC receptors differs strikingly from that for currents through muscle nicotinic receptors, which appear as of hundreds of events in quick succession over a range of high ACh concentrations.

ACh nevertheless elicits short bursts of several openings in quick succession through individual $\alpha7$–5HT$_{3A}$ HC receptors, and these bursts increase in number with increasing ACh concentration. We counted the number of such bursts of activity within the first minute of several recordings and found that bursts represented 23.8 $\pm$ 6% of the total opening events at 100 μM ACh ($n = 4$), and 41.8 $\pm$ 8% at 1 mM ACh ($n = 4$). The number of bursts elicited by 30 μM ACh was too low for quantitative comparison. However, the mean burst duration and number of openings per burst were indepen-
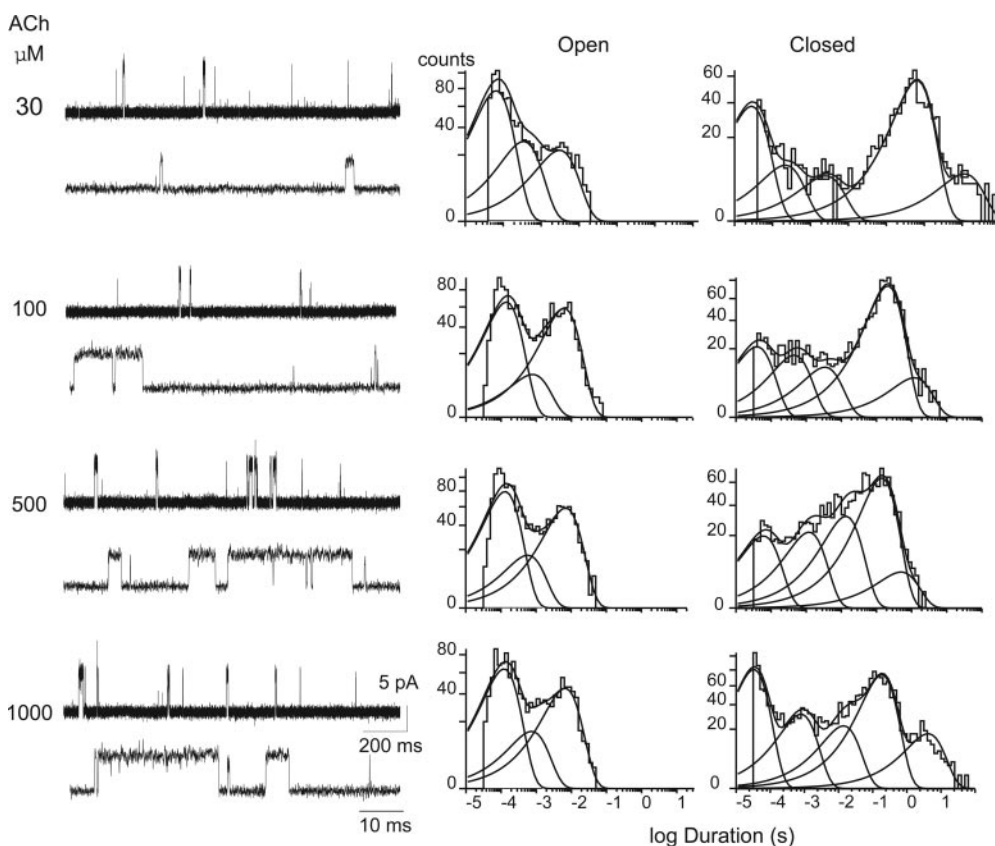
Fig. 4. $\alpha7$–5HT$_{3A}$ HC receptors activated by different concentrations of ACh. Traces of single channel activity at the indicated ACh concentrations are shown filtered at 8 kHz with channel openings as upward deflections. Corresponding open and closed time histograms are fitted by the sum of exponential components. Membrane potential, -70 mV.

TABLE 1

Properties of bursts as a function of agonist and concentration

Bursts were identified as a series of closely spaced events preceded and followed by closed intervals longer than a critical duration, which was taken as the point of intersection of the second and third closed time components (see Fig. 4). After selection of bursts, open, closed, and burst duration histograms were constructed. Only bursts with three or more openings were included in the analysis. Open and closed duration histograms are fitted by two components (O1/O2 and C1/C2 for open and closed time histograms, respectively). Results are shown as mean $\pm$ S.D. of at least three different patches for each condition.

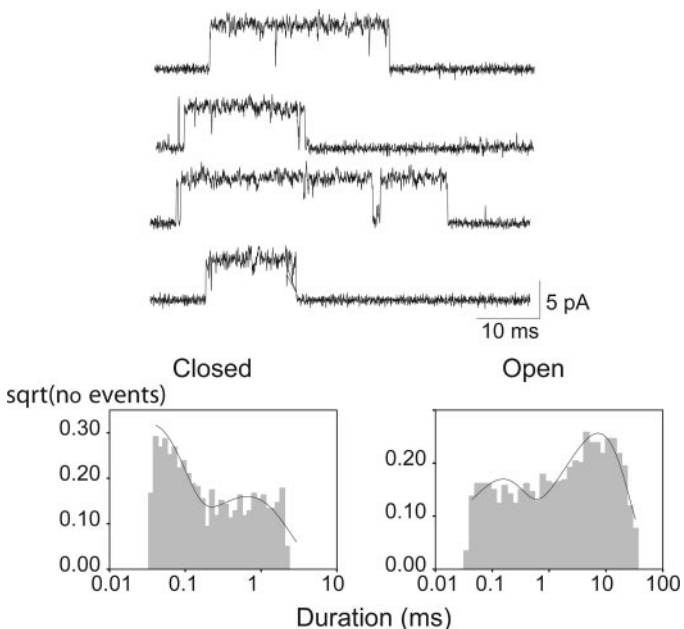| Agonist	P_{open}	O1 (Area)	O2 (Area)	C1 (Area)	C2 (Area)	τ Burst	Events/Burst
		ms				*ms*	
0.05 mM ACh	0.95 $\pm$ 0.01	0.13 $\pm$ 0.01 (0.25 $\pm$ 0.03)	3.1 $\pm$ 0.3 (0.74 $\pm$ 0.03)	0.02 $\pm$ 0.001 (0.87 $\pm$ 0.04)	0.51 $\pm$ 0.04 (0.13 $\pm$ 0.04)	16 $\pm$ 5.5	6.2 $\pm$ 0.3
0.1 mM ACh	0.96 $\pm$ 0.01	0.20 $\pm$ 0.02 (0.19 $\pm$ 0.04)	4.4 $\pm$ 0.5 (0.80 $\pm$ 0.04)	0.02 $\pm$ 0.007 (0.88 $\pm$ 0.04)	0.44 $\pm$ 0.12 (0.11 $\pm$ 0.04)	15.1 $\pm$ 3.1	4.2 $\pm$ 0.5
1 mM ACh	0.95 $\pm$ 0.01	0.07 $\pm$ 0.01 (0.33 $\pm$ 0.08)	5.7 $\pm$ 0.9 (0.67 $\pm$ 0.09)	0.03 $\pm$ 0.007 (0.85 $\pm$ 0.02)	0.52 $\pm$ 0.05 (0.14 $\pm$ 0.02)	17.6 $\pm$ 1.5	5.4 $\pm$ 1.8
0.05 mM Nic	0.95 $\pm$ 0.01	0.11 $\pm$ 0.08 (0.16 $\pm$ 0.02)	3.8 $\pm$ 0.39 (0.83 $\pm$ 0.03)	0.04 $\pm$ 0.007 (0.79 $\pm$ 0.01)	0.43 $\pm$ 0.07 (0.2 $\pm$ 0.01)	11.7 $\pm$ 3.2	3.4 $\pm$ 0.3
10 mM Choline	0.92 $\pm$ 0.05	0.15 $\pm$ 0.05 (0.41 $\pm$ 0.02)	2.9 $\pm$ 1.12 (0.58 $\pm$ 0.03)	0.02 $\pm$ 0.001 (0.85 $\pm$ 0.06)	0.45 $\pm$ 0.03 (0.14 $\pm$ 0.06)	10.3 $\pm$ 3.02	4.9 $\pm$ 1.0

P_{open}, channel open probability; τ_{burst}, mean burst duration obtained from the corresponding histogram.

dent of the ACh concentration (Table 1). These kinetic features indicate the short bursts correspond to activation of single $\alpha 7$–$5HT_{3A}$ HC receptors in which ACh is bound to multiple binding sites. The number of occupied binding sites could be as few as two and as many as five.
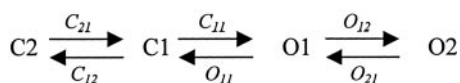
Because short bursts of openings represent the majority of current flow through $\alpha 7$–$5HT_{3A}$ HC receptors, we analyzed the corresponding open and closed intervals to gain insight into the kinetics of activation. We confined the analysis to bursts of openings elicited by 1 mM ACh to ensure saturation of the binding sites. For each recording, kinetic homogeneity of the bursts was ensured by selecting bursts with mean open durations and open probabilities within 2 S.D. of the corresponding means (see *Materials and Methods*).

To analyze burst kinetics, we first constructed closed and open time histograms and fitted them by the sum of exponential components. Both the open and closed time distributions are well described by the sum of two exponentials, indicating brief and long openings and closings within each burst (Table 1). We then inspected individual bursts to determine whether the brief and long openings and closings occurred randomly or in a preferred sequence. Long openings were mainly preceded and followed by brief closings but were sometimes flanked by long closings. Brief openings were mainly bounded by long closings but were sometimes flanked by brief closings. Thus the two classes of openings and closings seem to occur in any sequence (Fig. 5).

Among possible kinetic schemes, those that depict a linear sequence of alternating closed and open states do not account for the observation that the two classes of openings and closings can occur in any sequence. However, the linear Scheme 1, with consecutive closed and open states, could be fitted to the dwell times. Although the fitted rate constants (Table 2) account for the preference of long openings to be bounded by brief rather than long closings, they predict a preference of brief openings to be bounded by brief rather than long closings, contrary to the observations. Furthermore, the fraction of brief openings is predicted to be similar to that for long openings, again contrary to the observations.

We therefore examined a cyclic scheme for its ability to describe the data (Scheme 2). Channel block by ACh is not incorporated into Scheme 2 because the concentration of ACh is 1 mM, and the dissociation constant for block is 40 mM. To obtain realistic rate constants during fitting, the set of rate constants was required to satisfy the principle of microscopic reversibility. Maximum likelihood fitting of Scheme 2 to the set of closed and open intervals adequately describes the data, with computed probability density functions that overlay the dwell time histograms (Fig. 5 and Table 2). A branched scheme lacking the connection between states O2 and C2 could also describe the data, with the retained rate constants similar to those in Scheme 2, but does not account for the observation that long openings can be flanked by long closings.

Once the receptor has bound agonist, activation takes place as described by Scheme 2. Although the point of entry of agonist binding is not specified in Scheme 2, studies of

Fig. 5. Kinetics of activation of $\alpha 7$–$5HT_{3A}$ HC receptors. Single-channel activation episodes elicited by 1 mM ACh filtered at 8 kHz. Open and closed duration histograms are shown with probability density functions derived from fitting scheme 2 to open and closed intervals (smooth curves).

Scheme 1. The long closed state C2 connects with the brief closed state C1, which connects with the brief open state O1 in series with the long open state O2.

TABLE 2

Kinetic parameters for $\alpha 7$–5HT3

Values are results of simultaneous fits of Schemes 1 and 2 to data from three different patches in the presence of 1 mM ACh. For Scheme 1, the log likelihood was 13,571, whereas that for Scheme 2 was 13,621. Data are expressed as seconds^{-1}.

| Scheme 1	
C_{21}	2200 ± 116
C_{12}	6900 ± 440
C_{11}	$40,500 \pm 5000$
O_{11}	$11,000 \pm 2500$
O_{12}	7600 ± 940
O_{21}	424 ± 29
Scheme 2	
β_1	$10,400 \pm 1700$
α_1	7800 ± 1000
β_2	$37,500 \pm 3000$
α_2	330 ± 24
β_{12}	1500 ± 120
α_{12}	6100 ± 760
β_{22}	540 ± 70
α_{22}	25 ± 3
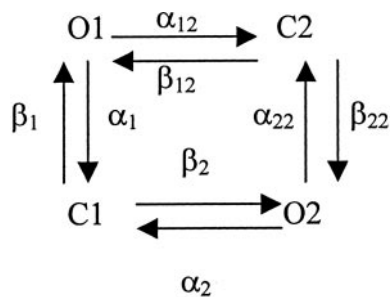
Scheme 2. Each open state is connected to two closed states, and vice versa. Because ACh is present at a saturating concentration, each state is assumed to have the maximum number of binding sites occupied by the agonist. The maximum number of occupied sites per receptor is not known but could be any number from two to five.

muscle nicotinic receptors show that a brief, fully occupied closed state precedes the open state, suggesting one of the two closed states is the point of entry. The choice of closed state can be determined, in principle, from the rate of current increase after a step pulse of a saturating concentration of agonist, which equals the sum of the rate constants leading away from that state. Our experiments rapidly applying ACh to outside-out patches gave a rate of rise as fast as 2000 s^{-1}, but this rate is a lower limit, because it is approximately the same as the intrinsic rate of solution exchange of our system. The sum of the rate constants leading away from either the long or the brief closed states is large enough to account for the observed rate of current rise. However, if the point of entry is assumed to be the state to which the long-lived open state closes with highest probability, the point of entry is the brief closed state (C1 in Scheme 2). Given this assumption, the $\alpha7-5HT_{3A}$ HC receptor opens its channel very rapidly upon ACh occupancy $(37,000 \text{ s}^{-1})$, similar to the rate of channel opening determined for muscle nicotinic receptors $(40,000-60,000 \text{ s}^{-1})$, and the channel closes after several milliseconds. Once fully occupied, the receptor opens and closes several times before the burst is terminated by desensitization. Our outside-out patch experiments show the time constant of current decay is similar to the mean burst dura-tion, indicating the overall response to agonist is determined by both activation and desensitization processes.

Single-Channel Currents Evoked by Nicotine and Choline. Single-channel currents are readily detected in the presence of (±)-nicotine concentrations as low as 5 μM (Fig. 6), as expected from the greater potency of nicotine in dose-response measurements (Fig. 1). Open time distributions are well described by the sum of three exponential components whose durations are similar to those obtained for ACh. At 100 μM nicotine, the mean open times and fractional areas are $\tau_1 = 150 \pm 30$ μs (0.37 ± 0.07), $\tau_2 = 1.6 \pm 0.7$ ms (0.19 ± 0.02), and $\tau_3 = 5.1 \pm 1$ ms (0.43 ± 0.03). In the presence of 5 μM nicotine, the fractional area of the slowest component is less than 0.1, indicating a reduced frequency of long channel openings in quick succession, as observed for ACh. High concentrations of nicotine block the channel, leading to a reduction in channel amplitude and mean open time (Fig. 6a).

Relatively high concentrations of choline are required to elicit single channel currents through $\alpha7-5HT_{3A}$ HC receptors, with the threshold for detection being approximately 200 μM (Fig. 6b). Open time distributions are well described by the sum of three exponential components whose durations are similar to those obtained for ACh and nicotine. In the
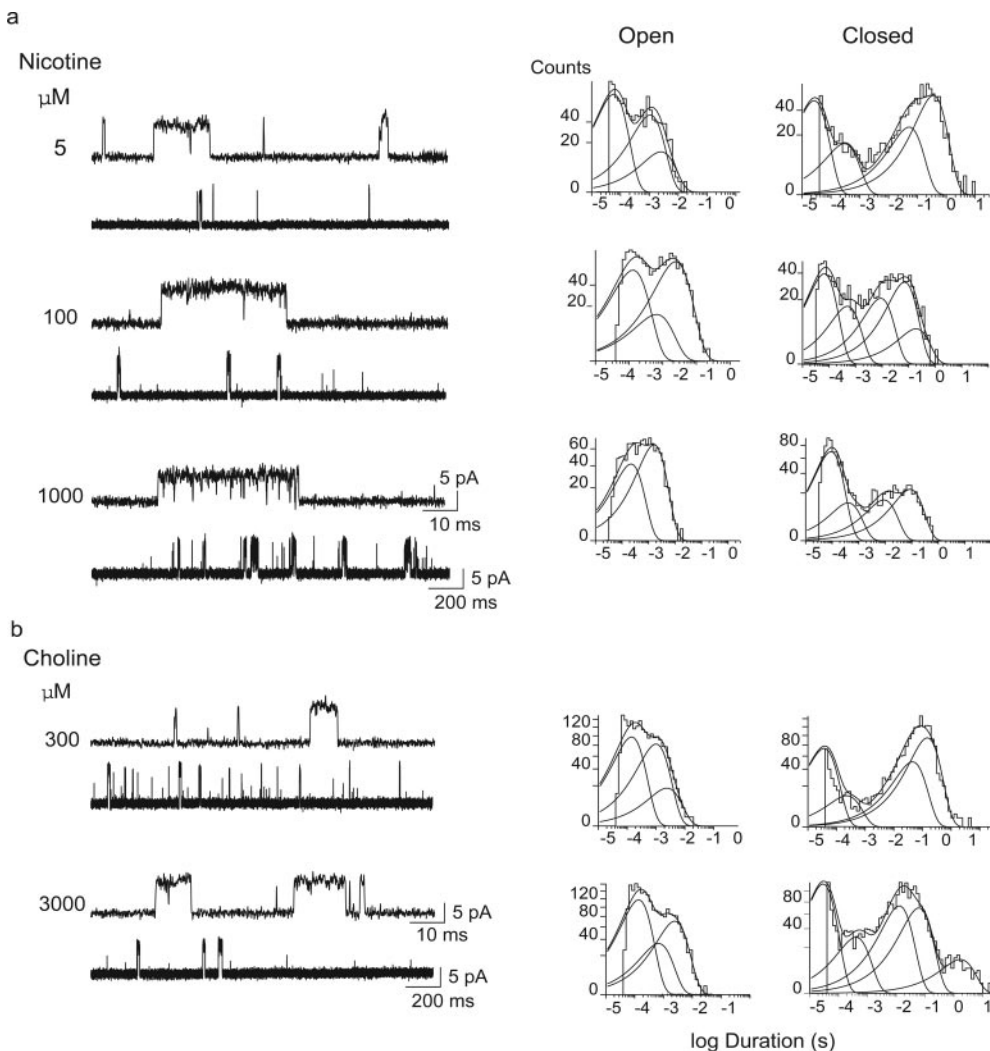
Fig. 6. $\alpha7-5HT_{3A}$ HC receptors activated by nicotine and choline. Traces of single channel activity elicited by nicotine (a) and choline (b) are shown filtered at 8 kHz with channel openings as upward deflections. Corresponding open and closed time histograms are shown fitted by the sum of exponential components. Membrane potential, −70 mV.

presence of 1 mM choline, the mean open times and fractional areas are $\tau_1 = 120 \pm 40$ μs (0.45 ± 0.10), $\tau_2 = 1.17 \pm 0.32$ ms (0.27 ± 0.14), and $\tau_3 = 5.10 \pm 1.9$ ms (0.34 ± 0.10). Bursts of several openings in quick succession are observed at concentrations of choline greater than 300 μM. Thus, although ACh, nicotine, and choline differ in their potency for activating the HC form of the $\alpha7$–$5HT_{3A}$ receptor, the channel gating kinetics are similar among the three agonists.

Discussion

Given the importance of $\alpha7$ receptors in a variety of normal and pathological processes and as targets for pharmacological agents (Gotti and Clementi, 2004), the kinetics of activation by agonist are of considerable interest. Because the $\alpha7$–$5HT_{3A}$ chimera expresses in robust quantities in mammalian cells, it has become a model system for pharmacological studies aimed at probing the ligand binding region of $\alpha7$. However, because of the low conductance conferred by the $5HT_{3A}$ portion of the chimera, single-channel events could not be resolved. By mutating determinants of channel conductance in the M3-M4 cytoplasmic linker, we were able to detect single channel currents and study the kinetics of activation of this widely used chimera.

The EC_{50} and apparent dissociation constant for ACh binding for the HC form of $\alpha7$–$5HT_{3A}$ are similar to those of the LC form, showing that the triple mutation in the M3-M4 linker does not affect macroscopic activation properties. The relative potencies of nicotinic agonists are similar to those reported for $\alpha7$ AChRs (Amar et al., 1993; Brammar, 1996), suggesting that the $\alpha7$–$5HT_{3A}$ HC chimera is a good model to study mechanisms of activation and modulation of $\alpha7$ AChRs.

Rapid application of ACh to cell-free patches shows that $\alpha7$–$5HT_{3A}$ HC receptors desensitize within several milliseconds, similar to $\alpha7$ receptors expressed in oocytes (Conroy et al., 2003). By contrast, $5HT_{3A}$ receptors desensitize with a double exponential time course with time constants of approximately 170 ms and 1 s (Mott et al., 2001). Therefore, the rate of desensitization onset seems to be determined by the extracellular rather than the pore region of the chimera. Analysis of the kinetics of desensitization indicates the rate of onset is comparable with the rate of channel closing, whereas the rate of recovery is some 10-fold slower. Our data show a major closed time component with a time constant of approximately 100 ms (Fig. 4), which agrees with the rate of recovery from desensitization ($1/10$ s^{-1}) computed from macroscopic currents.

Previous studies of muscle nicotinic receptors showed a majority of brief openings correspond to receptors with one bound agonist, whereas long openings correspond to receptors with two bound agonists (Colquhoun and Sakmann, 1985; Jackson, 1988; Papke et al., 1988; Milone et al., 1997). We find a small decrease in the fraction of brief openings when the ACh concentration is increased from 30 to 100 μM, indicating some brief openings correspond to receptors with fewer occupied sites than are required for optimal activation. However, brief openings are also found within bursts of long openings elicited by saturating concentrations of agonist, indicating brief openings can occur with multiple site occupancy, as found for fetal mouse muscle receptors in BC3H-1 cells (Sine and Steinbach, 1987). Openings with intermediate durations are observed at all agonist concentrations but are not found within bursts, suggesting that these represent an alternative but minor kinetic mode with an unspecified number of sites occupied. Bursts of long openings in quick succession appear at all agonist concentrations, and the frequency of such bursts increases as the agonist concentration is increased. Thus, the majority of current flows during bursts of long openings, indicating these correspond to receptors with the maximum number of occupied sites required for full activation.

To derive rate constants underlying activation by ACh, we analyzed open and closed intervals within bursts according to a scheme containing two open and two closed states. Because inspection of bursts shows that both brief and long openings are bounded by brief and long closings, and that long openings are frequently bounded by brief closings, whereas brief openings are frequently bounded by long closings, we fitted the cyclic Scheme 2 to data obtained in the presence of 1 mM ACh. Maximum likelihood fitting shows that Scheme 2 adequately describes the data, as judged by the coincidence between the predicted probability density functions and the dwell time histograms. Analysis of two-dimensional dwell-time distributions and dependence plots constitutes a means of quantitatively establishing state connectivity (Rothberg and Magleby, 1999).

Because closed intervals within bursts do not depend on ACh concentration, our data cannot yield rate constants for the agonist binding steps. However, the final agonist binding step should connect to one of the two closed states in Scheme 2. If the connection were to C2, transition to the long O2 state would be relatively slow and occur with low probability or would be reached through a secondary pathway via the brief open (O1) and closed (O2) states. However, the collective data suggest C1 is the most likely state linking binding to channel opening steps because 1) our outside-out patch experiments show the rate of channel opening is 2000 s^{-1} or faster, 2) long openings mediate the vast majority of current flow, and 3) long openings preferentially close to the C1 state. Thus, after agonist occupancy, transition from C1 to O2 is expected to produce rapid and efficient channel opening; the opening rate is estimated to be 37,000 s^{-1}, and the corresponding gating equilibrium constant, β_2/α_2, is 110.

The pattern of channel activity for $\alpha7$–$5HT_{3A}$ HC receptors was unexpectedly independent of agonist concentration. Channel events appear as single openings or as bursts of several openings in quick succession, and closed intervals within bursts do not depend on agonist concentration This bursting pattern differs strikingly from that for muscle nicotinic AChRs, which at high ACh concentrations activate in episodes of hundreds of openings in quick succession (Ogden and Colquhoun, 1983; Sine and Steinbach, 1987); within such episodes, closed intervals become progressively briefer with increasing ACh concentrations (Sine and Steinbach, 1987; Sine et al., 1990; Bouzatet al., 2000, 2002). For $\alpha7$–$5HT_{3A}$ HC receptors in the presence of a saturating concentration of agonist, rates of channel closing and desensitization are comparable. Thus, once the long open state is reached, the channel either closes or desensitizes. If the channel desensitizes, the burst is terminated; if it closes, dissociation of ACh is effectively prevented by the saturating concentration of ACh and another cycle of opening is initiated. Thus the number of openings per burst is given by (1 + channel closing rate/

desensitization rate), which equals 4.1 given our fitted parameters, in good agreement with the observed range of 3 to 6 openings per burst (Table 1). At subsaturating concentrations of agonist, however, the probability that the agonist will dissociate and rebind is high only if the rate of dissociation is comparable with the rate of channel opening. Our observation that the number of openings per burst and the intraburst closed times are concentration-independent indicates the rate of ACh dissociation is slow compared with the rate of channel opening. Thus, the response of $\alpha 7$–5HT$_{3A}$ HC receptors to agonist is governed jointly by the kinetics of channel gating and desensitization, which may have mechanistic implications for other homomeric Cys-loop receptors.

Acknowledgments

References

Amar M, Thomas P, Johnson C, Lunt GG, and Wonnacott S (1993) Agonist pharmacology of the neuronal a7 nicotinic receptor expressed in *Xenopus* oocytes. *FEBS Lett* **3:**284–288.

Bouzat C, Barrantes F, and Sine S (2000) Nicotinic receptor fourth transmembrane domain: hydrogen bonding by conserved threonine contributes to channel gating kinetics. *J Gen Physiol* **115:**663–672.

Bouzat C, Bren N, and Sine SM (1994) Structural basis of the different gating kinetics of fetal and adult nicotinic acetylcholine receptor. *Neuron* **13:**1395–1402.

Bouzat C, Gumilar F, Esandi MC, and Sine SM (2002) Subunit-selective contribution to channel gating of the M4 domain of the nicotinic receptor. *Biophys J* **82:**1920–1929.

Bouzat C, Gumilar F, Spitzmaul G, Wang HL, Rayes D, Hansen S, Taylor P, and Sine S (2004) Coupling of agonist binding to channel gating in an ACh-binding protein linked to ion channel. *Nature (Lond)* **430:**896–900.

Brammar W (1996) Nicotinic acetylcholine-gated integral receptor-channels, in *Ion Channel Facts Book 1* (Conley EC ed) pp 234–292, Academic Press, London.

Colquhoun D and Sakmann B (1985) Fast events in single-channel currents activated by acetylcholine and its analogues at the frog muscle end-plate. *J Physiol* **369:**501–557.

Conroy WG, Liu Q-S, Nai Q, Margiotta JF, and Berg DK (2003) Potentiation of α7-containing nicotinic acetylcholine receptors by select albumins. *Mol Pharmacol* **63:**419–428.

Corringer P-J, Bertrand S, Bohler S, Edelstein S, Changeux JP, and Bertrand D (1998) Critical elements determining diversity in agonist binding and desensitization of neuronal nicotinic acetylcholine receptors. *J Neurosci* **18:**648–657.

Drisdel R, Manzana E, and Green W (2004) The role of palmitoylation in functional expression of nicotinic alpha 7 receptors. *J Neurosci* **24:**10502–10510.

Eisele J-L, Bertrand S, Galzi J-L, Devillers-Thiery A, Changeux J-P, and Bertrand D (1993) Chimaeric nicotinic-serotoninergic receptor combines distinct ligand binding and channel specificities. *Nature (Lond)* **366:**479–483.

Fucile S, Palma E, Mileo AM, and Eusebi F (2000) Human neuronal threonine-for-leucine-248 a7 mutant nicotinic acetylcholine receptors are highly Ca^{2+} permeable. *Proc Natl Acad Sci USA* **97:**3643–3648.

Gotti C and Clementi F (2004) Neuronal nicotinic receptors: from structure to pathology. *Prog Neurobiol* **74:**363–396.

Grosman C and Auerbach A (2000) Asymmetric and independent contribution of the second transmembrane segment 12′ residues to diliganded gating of acetylcholine receptor channels: a single-channel study with choline as the agonist. *J Gen Physiol* **115:**637–651.

Grutter T, Prado de Carvalho L, LeNovere N, Corringer PJ, Edelstein S, and Changeux J-P (2003) An H-bond between two residues from different loops of the acetylcholine binding site contributes to the activation mechanism of nicotinic receptors. *EMBO (Eur Mol Biol Organ) J* **22:**1990–2003.

Hamill OP, Marty A, Neher E, Sakmann B, and Sigworth FJ (1981) Improved patch-clamp techniques for high-resolution current recording from cells and cell-free membrane patches. *Pflueg Arch Eur J Physiol* **391:**85–100.

Jackson MB (1988) Dependence of acetylcholine receptor channel kinetics on agonist concentration in cultured mouse muscle fibres. *J Physiol* **397:**555–583.

Kelley S, Dunlop J, Kirkness E, Lambert J, and Peters JA (2003) A cytoplasmic region determines single-channel conductance in 5-HT3 receptors. *Nature (Lond)* **424:**321–324.

Kem WR, Mahnir VM, Papke RL, and Lingle CJ (1997) Anabaseine is a potent agonist on muscle and neuronal alpha-bungarotoxin-sensitive nicotinic receptors. *J Pharmacol Exp Ther* **283:**979–992.

Liu Y and Dilger JP (1991) Opening rate of acetylcholine receptor channels. *Biophys J* **60:**424–432.

Milone M, Wang HL, Ohno K, Fukudome T, Pruitt JN, Bren N, Sine SM, and Engel AG (1997) Slow-channel myasthenic syndrome caused by enhanced activation, desensitization and agonist binding affinity attributable to mutation in the M2 domain of the acetylcholine receptor alpha subunit. *J Neurosci* **17:**5651–5665.

Mott DD, Erreger K, Banke TG, and Traynelis SF (2001) Open probability of homomeric murine 5-HT3A serotonin receptors depends on subunit occupancy. *J Physiol* **535:**427–443.

Niu L, Vazquez W, Nagel G, Friedrich T, Bamberg E, Ostwald RE, and Hess GP (1996) Rapid chemical kinetic techniques for investigations of neurotransmitter receptors expressed in *Xenopus* oocytes. *Proc Natl Acad Sci USA* **93:**12964–12968.

Ogden D and Colquhoun D (1985) Ion channel block by acetylcholine, carbachol and suberyldicholine at the frog neuromuscular junction. *Proc R Soc Lond B Biol Sci* **225:**329–355.

Ogden DC and Colquhoun D (1983) The efficacy of agonists at the frog neuromuscular junction studied with single channel recording. *Pflueg Arch Eur J Physiol* **399:**246–248.

Palma E, Fucile S, Barabino B, Miledi R, and Eusebi F (1999) Strychnine activates neuronal α7 nicotinic receptors after mutations in the leucine ring and transmitter binding site domains. *Proc Natl Acad Sci USA* **96:**13421–13426.

Papke RL, Millhauser G, Lieberman Z, and Oswald RE (1988) Relationships of agonist properties to the single channel kinetics of nicotinic acetylcholine receptors. *Biophys J* **53:**1–10.

Papke RL and Thinschmidt JS (1988) The correction of alpha7 nicotinic acetylcholine receptor concentration-response relationships in *Xenopus* oocytes. *Neurosci Lett* **256:**163–166.

Qin F, Auerbach A, and Sachs F (1996) Estimating single-channel kinetic parameters from idealized patch-clamp data containing missed events. *Biophys J* **70:**264–280.

Quiram PA and Sine SM (1998) Structural elements in α-conotoxin ImI essential for binding to neuronal alpha7 receptors. *J Biol Chem* **273:**11001–11006.

Rothberg BS and Magleby KL (1999) Gating kinetics of single large-conductance Ca^{2+}-activated K^{+} channels in high calcium suggest a two-tiered allosteric gating mechanism. *J Gen Physiol* **114:**93–124.

Sachs F (1999) Practical limits on the maximal speed of solution exchange for patch clamp experiments. *Biophys J* **77:**682–690.

Sigworth F and Sine SM (1987) Data transformation for improved display and fitting of single-channel dwell time histograms. *Biophys J* **52:**1047–1052.

Sine SM, Claudio T, and Sigworth FJ (1990) Activation of Torpedo acetylcholine receptors expressed in mouse fibroblasts. Single channel current kinetics reveal distinct agonist binding affinities. *J Gen Physiol* **96:**395–437.

Sine SM, Kreienkamp HJ, Bren N, Maeda R, and Taylor P (1995) Molecular dissection of subunit interfaces in the acetylcholine receptor: identification of determinants of alpha-conotoxin M1 selectivity. *Neuron* **15:**205–211.

Sine SM and Steinbach JH (1984) Agonists block currents through acetylcholine receptor channels. *Biophys J* **46:**277–284.

Sine SM and Steinbach JH (1987) Activation of acetylcholine receptors on clonal mammalian BC3H-1 cells by high concentrations of agonist. *J Physiol* **385:**325–359.

Sine SM and Taylor P (1979) Functional consequences of agonist-mediated state transitions in the cholinergic receptor. *J Biol Chem* **254:**3315–3325.

Spitzmaul G, Dilger JP, and Bouzat C (2001) The noncompetitive inhibitor quinacrine modifies the desensitization kinetics of muscle acetylcholine receptors. *Mol Pharmacol* **60:**235–243.

Williams M, Burton B, Urrutia A, Shcherbatko A, Chavez-Noriega L, Cohen C, and Aiyar J (2005) Ric 3 promotes functional expression of the nicotinic acetylcholine receptor a$_7$ subunit in mammalian cells. *J Biol Chem* **280:**1257–1283.

Address correspondence to: Cecilia Bouzat, Instituto de Investigaciones Bioquímicas, Camino La Carrindanga Km 7, 8000 Bahía Blanca, Argentina. E-mail: inbouzat@criba.edu.ar